Interplay between Turing Pattern Formation and Domain Coarsening in Spatially Extended Population Models

Hiroki SAYAMA[1,2]*, Marcus A. M. DE AGUIAR[1,3], Yaneer BAR-YAM[1,4] and Michel BARANGER[1,5]

[1]*New England Complex Systems Institute, Cambridge, MA 02138, U.S.A.*
[2]*Department of Human Communication, University of Electro-Communications,*
Chofu, Tokyo 182-8585, Japan
[3]*Instituto de Física 'Gleb Wataghin', Universidade Estadual de Campinas,*
13081-970, Campinas, São Paulo, Brazil
[4]*Department of Molecular and Cellular Biology, Harvard University, Cambridge, MA 02138, U.S.A.*
[5]*Physics Department, University of Arizona, Tucson, AZ 85721, U.S.A.*
E-mail address: sayama@hc.uec.ac.jp

Abstract. We introduce a model of spatially distributed populations of organisms that mate and compete with others in local neighborhoods. Competition for local finite resources causes Turing instability in population distribution, possibly leading to the formation of isolated groups. In the presence of disruptive selection against genetic intermediates, this model also shows dynamically coarsening domains in genetic distribution. We examine an interplay of these two distinct dynamics, both analytically and numerically, and show that the domain coarsening process is strongly affected by the spatial separation between groups created by the Turing pattern formation process. The ratio between mating and competition ranges is found to be one of the crucial parameters to determine the long-term evolution of genetic distribution in the population.

1. Introduction

The dynamics of spontaneous pattern formation, first introduced to biology by TURING (1952) five decades ago, has recently been attracting attention in many subfields of biology to describe various general and/or specific phenomena. Besides Turing's static patterns that arise when a homogeneous solution is unstable only for a limited range of wavelengths, there are other classes of pattern formation whose range of instability is not bounded, leading to scaling growth of patterns with time. Such dynamic patterns in a two-dimensional space have recently been introduced into ecology (LEVIN and SEGEL, 1985; GANDHI *et al.*, 1998, 1999) and evolutionary genetics (SAYAMA *et al.*, 2000, 2003). Most of the results obtained in these kinds of studies can be approximately described with a single non-conserved order parameter (e.g. type of organisms). They typically result in several well-known system behavior such as symmetry breaking and domain coarsening,

19

or nucleation and growth, depending on fitness assignments and initial conditions.

Here we consider a more general case that includes both static and dynamic pattern formation processes within a single model framework. The model we present pairs population distribution and genetic distribution of organisms. The underlying dynamics of our model correspond to the formation of isolated groups through population distribution variation and, in the presence of disruptive selection, symmetry breaking and domain coarsening through genetic distribution variation. We study the regimes in which patterns form and the characteristic wavelengths of the patterns, using linear stability analysis. Numerical simulations confirm these analytical results, and furthermore, demonstrate how the domain coarsening behavior interacts with Turing pattern formation. The ratio of the two key length scales in the problem, the mating range and the competition range, is found to be crucial in the long-term evolution of the patterns.

2. Model

We model a population with local genetic mixing by sexual reproduction and local competition for finite resources necessary for reproduction. We restrict ourselves to simple haploid genetics where a genome is made of two genes, each of which is one of two allelic types (+ and −) and is inherited from one of the two parents participating in sexual reproduction. Thus there are four possible genotypes, [++], [+−], [−+] and [−−]. Such organisms are distributed over a two-dimensional discrete regular spatial grid. At each discrete time step (breeding season), offspring are born and part of the previous population dies. Reproduction requires comsumption of local resources that are limited per site per season, so that it bounds the total number of offspring born there. Genetic mixing by sexual reproduction and competition for limited resources take place within local neighborhoods ranging over several sites, whose size may be different from one another.

The general form of the iterative equation of local populations on each site is

$$n'_{ab}(\boldsymbol{x}) = \sigma_{ab} n_{ab}(\boldsymbol{x}) + \lambda_{ab} \langle n(\boldsymbol{x}) \rangle_M \frac{\langle n_{a*}(\boldsymbol{x}) \rangle_M}{\langle n(\boldsymbol{x}) \rangle_M} \frac{\langle n_{*b}(\boldsymbol{x}) \rangle_M}{\langle n(\boldsymbol{x}) \rangle_M} \left[1 - \frac{\langle n(\boldsymbol{x}) \rangle_C}{\kappa} \right], \tag{1}$$

where $n_{ab}(\boldsymbol{x})$ (a, b are either + or −) is the local population of genotype [ab] at site $\boldsymbol{x}$, with the constraint $n_{ab} \geq 0$. We also use the following notations:

$$n \equiv n_{++} + n_{+-} + n_{-+} + n_{--}, \tag{2}$$

$$n_{a*} \equiv n_{a+} + n_{a-}, \tag{3}$$

$$n_{*b} \equiv n_{+b} + n_{-b}. \tag{4}$$

The prime on the left hand side of Eq. (1) denotes the value after a unit of time. σ_{ab} is the survival rate of parents of genotype [ab], and λ_{ab} is their reproductive rate (the number of

offspring born per parent per season). These rates are bounded so that $0 < \sigma_{ab} < 1$ and $\lambda_{ab} > 0$. M is the mating neighborhood, and C is the competition neighborhood. We assume that M and C are a set of relative coordinates of sites in a pseudo-circular region centered at the site, whose radius is R_M or R_C and whose edges are jagged (not a perfect circle) along a discrete square spatial lattice. κ is the carrying capacity per site. Each pair of angled brackets in the right hand side represent the local average of the given function in the neighborhood around x, i.e.

$$\langle f(\boldsymbol{x}) \rangle_N \equiv \left[\sum_{\boldsymbol{r} \in N} f(\boldsymbol{x} + \boldsymbol{r}) \right] \Big/ |N|, \tag{5}$$

where $|N|$ is the number of sites included in the neighborhood N. The terms inside the square brackets on the right hand side of Eq. (1) describe a logistic growth restriction on the population at local sites due to the already existing population in their vicinity.

Equation (1) implies that if the limitation on population by competition is ignored, $(1 - \sigma)$ of the population at a particular site will die and λ of the average population within its local mating neighborhood will be born in each breeding season. The genetic composition of the newborns is determined in Eq. (1) by including the product of two allelic probabilities observed within the mating neighborhood. For more details of the model we refer to SAYAMA *et al.* (2002).

3. Turing Pattern Formation in Population Distribution

If there is no difference in fitness (reproduction and survival rates) among all the four genotypes, i.e., $\sigma_{ab} = \sigma$ and $\lambda_{ab} = \lambda$ for all a and b, then summing up both sides of Eq. (1) for all genotypes gives

$$n'(\boldsymbol{x}) = \sigma n(\boldsymbol{x}) + \lambda \langle n(\boldsymbol{x}) \rangle_M \left[1 - \langle n(\boldsymbol{x}) \rangle_C \right], \tag{6}$$

with the constraint $n \geq 0$. Here we measure the populations in units of the carrying capacity κ for simplicity. This is a simplified equation for the population distribution only, independent of genetic distribution, which we call the *flat fitness case*. In this case genetic distribution shows simple random diffusion because no selective force is acting for any particular genotype (SAYAMA *et al.*, 2002). We thus focus in this section on the dynamics of population distribution only. Mean field treatment of Eq. (6) gives two stationary solutions, $n = 0$ and $n = (\sigma + \lambda - 1)/\lambda \equiv n_0$.

To investigate the instability of Eq. (6), we consider a two-dimensional oscillatory perturbation added to n_0, with wavevector v for the x-direction and w for the y-direction. We write the time evolution of perturbation in a two-dimensional population as

$$n^t(x, y) = n_0 + \xi \mu^t s(x, y) \tag{7}$$

with

$$s(x, y) = \sin(vx + \phi)\sin(wy + \psi), \tag{8}$$

where ξ is a small amplitude. The mean field solutions are unstable and patterns form when μ is greater than 1. Substituting Eq. (7) into Eq. (6) and keeping only linear (first-order) terms of ξ, we obtain

$$n^{t+1}(x, y) = n_0 + \xi\mu^t\Big[\sigma s(x, y) + (1 - \sigma)\big\langle s(x, y)\big\rangle_M - (\sigma + \lambda - 1)\big\langle s(x, y)\big\rangle_C\Big]. \tag{9}$$

Approximating the averages over M and C using integrals over continuous circular neighborhoods gives

$$\big\langle s(x, y)\big\rangle_N \approx \frac{2s(x, y)J_1(fR_N)}{fR_N}, \tag{10}$$

where $f \equiv \sqrt{v^2 + w^2}$ is the magnitude of the two-dimensional wavevector, and J_n is the Bessel function of the first kind of order n (SAYAMA *et al.*, 2002). Applying this approximation to Eq. (9), we obtain

$$\mu = \sigma + (1 - \sigma)A(fR_M) - (\sigma + \lambda - 1)A(fR_C) \tag{11}$$

with

$$A(u) \equiv \frac{2J_1(u)}{u}. \tag{12}$$

This function has a conspicuous minimum at $u \approx 5.13562$ where $A(u) \approx -0.132279$, which we call u_0 and z_0 in what follows.

   The condition for instability of the mean field solutions is the existence of such values of u that satisfy

$$\delta A(u / \gamma) < A(u) - 1, \tag{13}$$

where $u \equiv fR_M$, $\gamma \equiv R_M/R_C$, and $\delta \equiv (\sigma + \lambda - 1)/(1 - \sigma)$. Here we use the following approximation: When parameters γ and δ gradually move from stable regimes, the value of u that first satisfies this inequality should be obtained near the minimum of its left hand side, at $u = \gamma u_0$ where $\delta A(u/\gamma) = \delta z_0$. With this assumption, the condition for the satisfiability of the inequality is
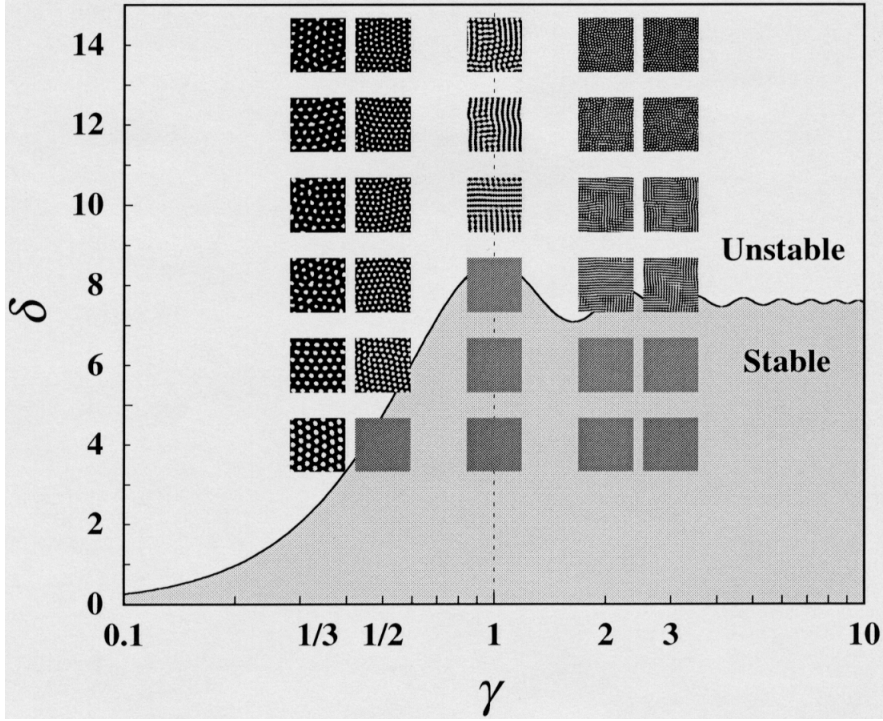
Fig. 1. Phase diagram in the (γ, δ) plane showing the stability of the mean field solution obtained from the inequality (14). In the shaded region below the curve, $\delta z_0 > A(\gamma u_0) - 1$, which implies that the mean field solution is stable, while above the curve it is not. Numerical simulation results for several sample points are embedded in the plot. Each picture embedded represents a snapshot of the evolution of spatial patterns taken after 500 updates. Initial conditions are randomly generated populations with $n = 0.1\kappa$ (with $\pm 0.02\kappa$ fluctuations) for each site. The space consists of 128×128 sites with periodic boundary conditions. The brightness at each pixel represents the local population density. σ is set to 0.9 for all cases. λ is varied to obtain different values of δ. The values of (R_M, R_C) used here are (5, 15) for $\gamma = 1/3$, (5, 10) for $\gamma = 1/2$, (10, 10) for $\gamma = 1$, (10, 5) for $\gamma = 2$, and (15, 5) for $\gamma = 3$.

$$\delta z_0 < A(\gamma u_0) - 1. \tag{14}$$

Figure 1 shows the regimes where this condition is, or is not, satisfied in the (γ, δ) plane. We see that, as the mating range becomes smaller than the competition range, the mean field solution can be destabilized, while if the mating range is greater than the competition range, the stability of the mean field solution is determined almost solely by δ. Numerical simulation results are embedded in the same figure for several different γ and δ, implying the close correspondence of our analysis to the actual model behavior. The existence of an instability is seen as the formation of isolated groups (spots or stripes) similar to those seen in Turing instability models (Turing, 1952; Murray, 1981; Young, 1984). Local

population growth and competition for resources within *C* in our model correspond to local activation and long-range inhibition factors of Turing pattern formation, respectively. We have calculated in SAYAMA *et al.* (2002), with the assumption $\delta >> 1$, the characteristic wavelength of the patterns *L* to be

$$L = \frac{2\pi R_C}{u_0} \approx 1.22345 R_C, \tag{15}$$

which coincides with the numerical results shown in Fig. 1. We have also found in the same literature that the genetic diffusion over isolated groups stops when the spatial separation is wider than the mating range of organisms. The critical ratio of the mating and competition ranges γ_c (below which groups become genetically decoupled after Turing pattern formation) is estimated be $\gamma_c \approx 0.612$ (SAYAMA *et al.*, 2002).

An interesting characteristic of the present model is its sensitivity to the shape of neighborhoods. The average of a function $f(\boldsymbol{x})$ over a neighborhood *N* can be written by

$$\langle f(\boldsymbol{x}) \rangle_N = \frac{\sum_{\boldsymbol{r}} f(\boldsymbol{x}+\boldsymbol{r}) W_N(\boldsymbol{r})}{\sum_{\boldsymbol{r}} W_N(\boldsymbol{r})}, \tag{16}$$

where $W_N(\boldsymbol{r})$ is a weight function. In the presented model we adopt "circular" neighborhoods, i.e. $W_N(\boldsymbol{r}) = 1$ if $|\boldsymbol{r}| < R_N$ and otherwise 0. We have tested other possibilities such as "square" neighborhoods or "Gaussian" neighborhoods. The square neighborhoods, obtained by re-defining $W_N(\boldsymbol{r}) = 1$ if $\max(|r_x|, |r_y|) < R_N$ and otherwise 0, give results similar to those with circular neighborhoods. However, this is not the case for the Gaussian neighborhoods with $W_N(\boldsymbol{r}) = e^{-(|\boldsymbol{r}|/R_N)^2}$. In this case, the mean field solution is stable against perturbation of any wavelength in population distribution, because the integral of sin functions with Gaussian weights, which is a Fourier transform, is again a Gaussian. This cannot be negative in contrast to the function $A(u)$. Therefore the average of the perturbation at a given point always has the same sign as the perturbation itself at that point. Even if the perturbation is very small, the average cannot reverse its sign and destructive interference cannot happen in population distribution, therefore spatial separation does not take place.

From a biological point of view, this result means that isolated groups may or may not form depending on the organismal territorial behavior. In particular, when the range of foraging or mating is well defined, groups may form. If they are too smooth, e.g. if organisms diffuse in a random fashion (which results in Gaussian neighborhoods), groups will not form. This prediction could, in principle, be verified experimentally.

4. Introduction of Disruptive Selection

In this section we introduce disruptive selection (selection against genetic intermediates) to the model, by assuming that genotypes [+−] and [−+] are not viable, i.e. $\sigma_{+-} = \sigma_{-+} = \lambda_{+-}$

$= \lambda_{-+} = 0$. Disruptive selection arises in various conditions in nature, such as competition for diverse resources or mutual dependence of multiple phenotypes (THODAY, 1972), and is viewed as one of the most general and important causes of inhomogeneity generation, including trait divergence and speciation (KONDRASHOV and KONDRASHOV, 1999; DIECKMANN and DOEBELI, 1999). This additional assumption reduces the number of viable genotypes to two, simplifying analytic treatments.

In what follows, we use g for n_{++} and h for n_{--} to make the notation concise. Similarly, the survival and reproductive rates for these types are denoted by σ_g, λ_g, σ_h, λ_h. We restrict ourselves to symmetric cases only, in which two viable genotypes g and h share the same survival and reproductive rates, i.e. $\sigma_g = \sigma_h = \sigma$ and $\lambda_g = \lambda_h = \lambda$. Finally, we again measure the populations in units of the carrying capacity κ. With these assumptions Eq. (1) becomes

$$g'(x) = \sigma g(x) + \frac{\lambda \langle g(x) \rangle_M^2}{\langle g(x) + h(x) \rangle_M} \Big[1 - \langle g(x) + h(x) \rangle_C \Big], \tag{17}$$

$$h'(x) = \sigma h(x) + \frac{\lambda \langle h(x) \rangle_M^2}{\langle g(x) + h(x) \rangle_M} \Big[1 - \langle g(x) + h(x) \rangle_C \Big], \tag{18}$$

with the constraints $g \geq 0$, $h \geq 0$. Mean field treatment of these equations gives the following four stationary solutions (SAYAMA et al., 2002):

- $g = h = 0$ (extinction)

- $g = \dfrac{\sigma + \lambda - 1}{\lambda} \equiv g_0, \quad h = 0$ (dominance by $[++]$)

- $g = 0, \quad h = \dfrac{\sigma + \lambda - 1}{\lambda} \equiv h_0$ (dominance by $[--]$)

- $g = h = \dfrac{2\sigma + \lambda - 2}{2\lambda} \equiv m_0$ (coexistence of the two).

Versions of this disruptive selection model have been used to study symmetry breaking and domain coarsening in spatially distributed populations (SAYAMA et al., 2000) and stability analysis of polymorphic populations in reproduction-migration dynamics among semi-isolated demes (DE AGUIAR et al., 2002).

We note that Eqs. (17) and (18) can be rewritten in terms of the local population, $n = g + h$, and what we call type difference, $c \equiv g - h$ ($-n \leq c \leq n$), i.e.

$$n'(\boldsymbol{x}) = \sigma n(\boldsymbol{x}) + \lambda \frac{\langle n(\boldsymbol{x})\rangle_M^2 + \langle c(\boldsymbol{x})\rangle_M^2}{2\langle n(\boldsymbol{x})\rangle_M}\Big[1 - \langle n(\boldsymbol{x})\rangle_C\Big], \tag{19}$$

$$c'(\boldsymbol{x}) = \sigma c(\boldsymbol{x}) + \lambda\langle c(\boldsymbol{x})\rangle_M\Big[1 - \langle n(\boldsymbol{x})\rangle_C\Big]. \tag{20}$$

We conduct a linear stability analysis of pattern formation in both population distribution and type difference for the disruptive selection case. We study the mixed solution only, because the dynamics of the one-type dominant solutions is the same as that of the flat fitness case due to their robustness against type difference perturbation, which can be verified by assuming $h << g \approx g_0$ (or $g << h \approx h_0$) in the mean field treatment of Eqs. (17) and (18). Adding a two-dimensional oscillatory perturbation to the mixed solution, we write

$$n^t(x, y) = 2m_0 + \zeta v^t s(x, y), \tag{21}$$

$$c^t(x, y) = 0 + \eta v^t s(x, y), \tag{22}$$

where ζ and η are small amplitudes and $s(x, y)$ is the same space-dependent perturbation (Eq. (8)) as used in the previous analysis. Substituting Eqs. (21) and (22) into Eqs. (19) and (20) and keeping only linear terms of ζ and η, the equations for these two variables decouple and we obtain

$$n^{t+1}(x, y) = 2m_0 + \zeta v^t\Big[\sigma s(x, y) + (1 - \sigma)\langle s(x, y)\rangle_M - (\sigma + \lambda / 2 - 1)\langle s(x, y)\rangle_C\Big], \tag{23}$$

$$c^{t+1}(x, y) = \eta v^t\Big[\sigma s(x, y) + 2(1 - \sigma)\langle s(x, y)\rangle_M\Big]. \tag{24}$$

Using the approximation in Eq. (10) for the local averages results in

$$v\zeta = \Big[\sigma + (1 - \sigma)A(fR_M) - (\sigma + \lambda / 2 - 1)A(fR_C)\Big]\zeta, \tag{25}$$

$$v\eta = \Big[\sigma + 2(1 - \sigma)A(fR_M)\Big]\eta, \tag{26}$$

with eigenvalues

$$v = \sigma + (1 - \sigma)A(fR_M) - (\sigma + \lambda/2 - 1)A(fR_C) \tag{27}$$

for eigenvector $(\zeta, 0)$, which we call the *n*-direction, and

$$\nu = \sigma + 2\,(1 - \sigma)A(\,fR_M) \tag{28}$$

for eigenvector $(0, \eta)$, which we call the c-direction.

Equation (27) is similar to Eq. (11), so we can apply the results of the previous stability analysis to the n-direction, by replacing δ with $\hat{\delta} \equiv (\sigma + \lambda/2 - 1)/(1 - \sigma)$. The regime for patterns to form in population distribution is thus exactly the same as shown in Fig. 1 if we view the ordinate as the $\hat{\delta}$ axis. The characteristic wavelength L is the same as before.

In terms of the c-direction, however, the eigenvalue ν depends only on σ, R_M, and not on λ, R_C. Considering $|\nu| > 1$ we obtain

$$A(\,fR_M) > \frac{1}{2}, \tag{29}$$

which numerically gives $fR_M < u_c \approx 2.21509$. This means that any perturbation in the c-direction whose wavelength is longer than the critical value

$$L_c \equiv 2\pi R_M/u_c \approx 2.83654 R_M \tag{30}$$

destabilizes the mean field solution. This is the direction of type difference, $g = -h$, increasing g while decreasing h, or the reverse. This result implies that all perturbations with shorter wavelengths than L_c are filtered out in an initial transient and then each local site tends to align with its neighbors at the scale L_c toward either genotype [++] or [−−].

Note that L_c only depends on the mating range and not on the competition range. This result is intuitive because it corresponds to the relevance of the mating range for genetic patterns and the competition range for population distribution variation. In the linear stability analysis, these two effects are found to be independent. However, an interplay between them arises once nonlinear effects become important. The details of this process will be discussed in the following.

5. Domain Coarsening in Genetic Distribution

We next consider the dynamics of genetic distribution in the disruptive selection case and how it is affected by the spatial population structure created by competition. We start by rewriting the model using the relative probabilities of genotypes. The update equation of the probability of one genotype can be obtained from Eqs. (19) and (20) by defining $p_g \equiv g/n = (n + c)/(2n)$ for sites where organisms exist ($n > 0$), which results in

$$p'_g(x) = p_g(x) + \frac{U(x)}{\sigma + U(x)}\left[\frac{\left(P_g^M(x)\right)^2}{\left(P_g^M(x)\right)^2 + \left(1 - P_g^M(x)\right)^2} - p_g(x)\right], \tag{31}$$

with

$$U(x) \equiv \frac{\lambda \langle n(x) \rangle_M}{n(x)} \Big[1 - \langle n(x) \rangle_C \Big] \Big[\big(P_g^M(x) \big)^2 + \big(1 - P_g^M(x) \big)^2 \Big], \tag{32}$$

$$P_g^M(x) \equiv \frac{\langle g(x) \rangle_M}{\langle n(x) \rangle_M} = \frac{\langle n(x) + c(x) \rangle_M}{2 \langle n(x) \rangle_M}. \tag{33}$$

$P_g^M(x)$ is the probability of genotype [++] observed within M around x. For populations that do not exceed the carrying capacity, $U(x)/[\sigma + U(x)]$ is always positive and thus p_g always approaches the first term in the square brackets. The above equations are for genotype [++] but they also apply to genotype [−−] due to the symmetry between the types.

The mean field version is

$$p_g' = p_g + \frac{U}{\sigma + U} \left[\frac{p_g^2}{p_g^2 + \big(1 - p_g \big)^2} - p_g \right]$$

$$= (1 - \chi) p_g + \chi \frac{p_g^2}{p_g^2 + \big(1 - p_g \big)^2}, \tag{34}$$

where $\chi \equiv U/[\sigma + U]$. This form shows that p_g tends to go toward either 0 or 1, depending on whether its current value is larger or smaller than 1/2. $p_g = 0$ and $p_g = 1$ are the only possible stable solutions. Thus, any change in the average genetic composition within the mating neighborhood will not significantly affect the future genetic composition at the center of the neighborhood, unless the change is great enough to move the average composition across the value 1/2. Therefore, the change of genetic composition due to the
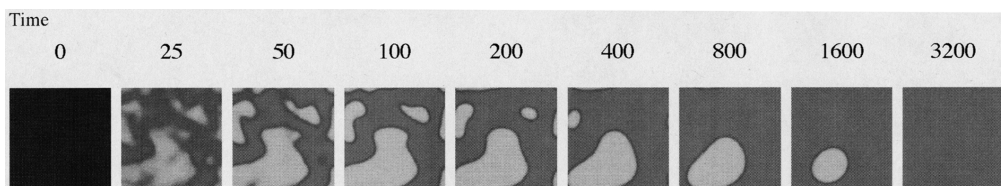
Fig. 2. Numerical simulation result of pattern formation in genetic distribution in the disruptive selection case. The space consists of 128×128 sites with periodic boundary conditions. Dark gray represents the existence of [++] organisms, while light gray represents the existence of [−−]. The initial condition is a randomly generated population with $n = 0.1\kappa$ (with $\pm 0.02\kappa$ fluctuations) for each site. $\sigma = 0.9$, $\lambda = 0.7$, $R_M = 5$ and $R_C = 3$, so that $\hat{\delta} = 2.5$ and $\gamma = 1.66667$. This parameter setting falls in the regime where the homogeneous population distribution is stable (see Fig. 1) and thus no spatial separation occurs. The observed behavior is symmetry breaking and domain coarsening, which is found in systems with non-conserved order parameters, such as quenched Ising models.

influx of different genotypes, or genetic invasion, can occur only if there is a sufficiently large bias imposed on the local genetic composition from neighboring areas.

Figure 2 shows a numerical simulation of this process with parameter settings for which the homogeneous population distribution is stable. Disruptive selection causes each local region to assume either of the two fittest types, giving rise to symmetry breaking and formation of patterns of two different genotypes (dark gray and light gray shown in the figure). Once the patterns form, their subsequent evolution follows well-known domain coarsening behavior in systems where the order parameter is not conserved (BRAY, 1994), e.g. quenched Ising models. The boundaries between the two types (called hybrid zones) move toward the direction determined by their local curvature, which acts as a bias on the local genetic composition. The characteristic wavelength of the patterns grows as $t^{1/2}$ (SAYAMA *et al.*, 2000). In general, a population of finite size will eventually be dominated by one of the two types. Such coarsening dynamics is consistent with the eigenvalue ν in the c-direction in Eq. (28), describing the instability of the mixed solution to type difference perturbations. The value of ν monotonically increases as the wavelength of the perturbations increases for $L > L_c$, indicating that larger scale perturbations become more apparent over longer times.

6. Domain Coarsening over Turing Patterns

For populations spontaneously structured into spatially isolated groups, the spatial separation between the groups significantly affects the genetic invasion processes. When such isolation occurs, the ratio of the mating and competition ranges, γ, determines the possibility of genetic invasion.

We systematically consider this problem by dividing the local population within the mating neighborhood into two parts: a particular group at the center of the neighborhood, and the set of other groups that are spatially separated from the central group. Each part is represented by its total population. In a sense, this characterization corresponds to a mean field approximation applied to the group-level description of the system. The total population and the probability of genotype [++] within the focal group are denoted by n_{en} and P_g^{en}, and similarly, those outside the group by n_{ex} and P_g^{ex}. We consider how the genetic composition of the focal group P_g^{en} develops over time, assuming P_g^{ex}, n_{en} and n_{ex} as environmental constants. In the context of domain coarsening in type difference, P_g^{ex} can be considered to represent the local curvature of boundaries between two types for the groups at or near the boundaries. This enables us to obtain implications for the domain coarsening behavior from this analysis.

We assume that each isolated group is genetically well mixed so that P_g^{en} is represented by the local probability p_g at the center of that group. From Eq. (31), p_g tends to approach $(P_g^M)^2/[(P_g^M)^2 + (1 - P_g^M)^2]$. The quantity P_g^M, the probability of genotype [++] within the neighborhood, is written as

$$P_g^M = \frac{P_g^{\text{ex}} n_{\text{ex}} + P_g^{\text{en}} n_{\text{en}}}{n_{\text{ex}} + n_{\text{en}}}$$

$$= P_g^{\text{ex}} d + P_g^{\text{en}} (1 - d), \tag{35}$$

where $d \equiv n_{\text{ex}}/[n_{\text{ex}} + n_{\text{en}}]$. The parameter d is the ratio of the subpopulation outside the focal group to the total population, within the neighborhood. Applying Eq. (35) to Eq. (31) and replacing p_g with $P_g{}^{\text{en}}$, we obtain a difference equation

$$\Delta P_g^{\text{en}} \equiv P_g^{\text{en}\,\prime} - P_g^{\text{en}}$$

$$= \frac{U}{\sigma + U} \times \left[\frac{\left(P_g^{\text{ex}}d + P_g^{\text{en}}(1-d)\right)^2}{\left(P_g^{\text{ex}}d + P_g^{\text{en}}(1-d)\right)^2 + \left(1 - P_g^{\text{ex}}d - P_g^{\text{en}}(1-d)\right)^2} - P_g^{\text{en}} \right]. \qquad (36)$$

To study the possibility of genetic invasion, we consider when stable solutions of $\Delta P_g{}^{\text{en}} = 0$ exist for particular $P_g{}^{\text{ex}}$ and d. We solve $\Delta P_g{}^{\text{en}} = 0$ with the restrictions $0 \le P_g{}^{\text{en}} \le 1$ and $0 \le P_g{}^{\text{ex}} \le 1$, which gives

$$P_g^{\text{en}} = 0, \ \frac{1}{2}, \ 1 \qquad (37)$$

for $d = 0$, or otherwise

$$P_g^{\text{ex}} = \begin{cases} P_g^{\text{en}} + \dfrac{2P_g^{\text{en}}\left(1 - P_g^{\text{en}}\right) - \sqrt{P_g^{\text{en}}\left(1 - P_g^{\text{en}}\right)}}{d\left(2P_g^{\text{en}} - 1\right)} & \left(\text{for } P_g^{\text{en}} \ne \dfrac{1}{2}\right) \\[2em] \dfrac{1}{2} & \left(\text{for } P_g^{\text{en}} = \dfrac{1}{2}\right), \end{cases} \qquad (38)$$

which forms a continuous function that is differentiable for $0 < P_g{}^{\text{en}} < 1$ including $1/2$. Figure 3 shows phase diagrams in the $(P_g{}^{\text{en}}, P_g{}^{\text{ex}})$ plane drawn from these solutions for different values of d. At $d = d_0$, a critical situation arises where the curve comes in contact with $P_g{}^{\text{ex}} = 0$ and $P_g{}^{\text{ex}} = 1$. At $d = d_1$, another critical situation is reached where the curve loses its unstable part. The actual values of d_0 and d_1 are analytically calculable, which results in $d_0 = 3 - 2\sqrt{2} \approx 0.171573$ and $d_1 = 1/2$.

From Fig. 3 we understand the following:

For $d = 0$:

The environment $P_g{}^{\text{ex}}$ has absolutely no effect on the genetic composition of the focal group.

For $0 < d < d_0$:

A group with $P_g{}^{\text{en}}$ close to $1/2$ is sensitive to $P_g{}^{\text{ex}}$. However, a group starting at or near $P_g{}^{\text{en}} = 0$ or 1 cannot change to the opposite type due to the existence of intermediate stable solutions. Once an isolated group approaches dominance by either of the two fittest genotypes, genetic shift from one type to another is not possible regardless of $P_g{}^{\text{ex}}$.

For $d_0 < d < d_1$:
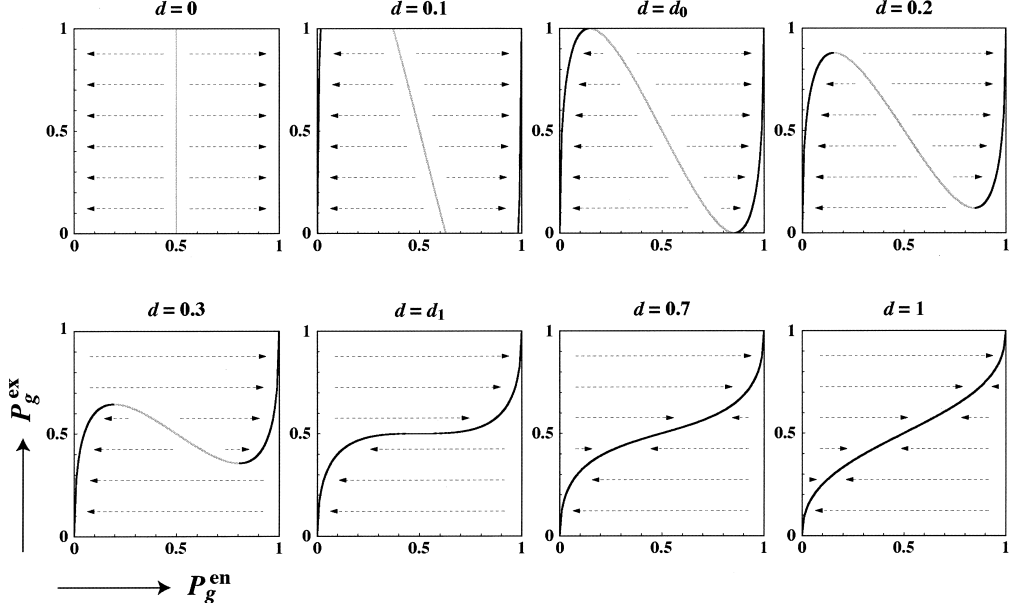
Fig. 3. Phase diagrams in the (P_g^{en}, P_g^{ex}) plane for different values of d, obtained from Eqs. (37) and (38). The curves represent the solutions of $\Delta P_g^{en} = 0$. Black parts of the curves are stable and gray parts are unstable. For $d < d_0$, a group starting at or near $P_g^{en} = 0$ or 1 remains close to its original state almost regardless of P_g^{ex}. For $d_0 < d < d_1$, genetic invasion is possible for sufficiently large (or small) P_g^{ex}. For $d > d_1$, genetic invasion always occurs since the final state of P_g^{en} is determined solely by P_g^{ex}, regardless of its original state. The actual values of d_0 and d_1 can be found analytically to be $d_0 = 3 - 2\sqrt{2} \approx 0.171573$ and $d_1 = 1/2$.

Genetic invasion is possible for P_g^{ex} larger (or smaller) than the local maximum (or minimum) of the curve. This indicates that the influx of a different genotype to the group must be greater than a threshold to cause genetic invasion. In the context of domain coarsening, boundaries whose local curvature is smaller than the threshold may be frozen, and in general will not become flat. The maximal curvature that can be kept from coarsening is determined by the values of P_g^{ex} at its extrema, which is a function of d. For $d_1 < d$:

P_g^{en} always converges toward a value determined solely by P_g^{ex}, regardless of its original state, thus genetic invasion always occurs. In the context of domain coarsening, any small curvature of boundaries can, in principle, give rise to change in genetic composition in the group at the boundaries, and coarsening continues until all the boundaries become flat or the entire population becomes dominated by one type.

The variable d is ultimately determined by the model parameter γ, the ratio of mating and competition ranges. For large γ, the mating neighborhood extends over more groups, which increases d as well. Although the exact value of d is hard to obtain, we estimate it by using the assumptions that (1) groups are arranged on a regular hexagonal grid (Fig. 4(a)) as seen in the numerical simulations, and that (2) the population distribution within
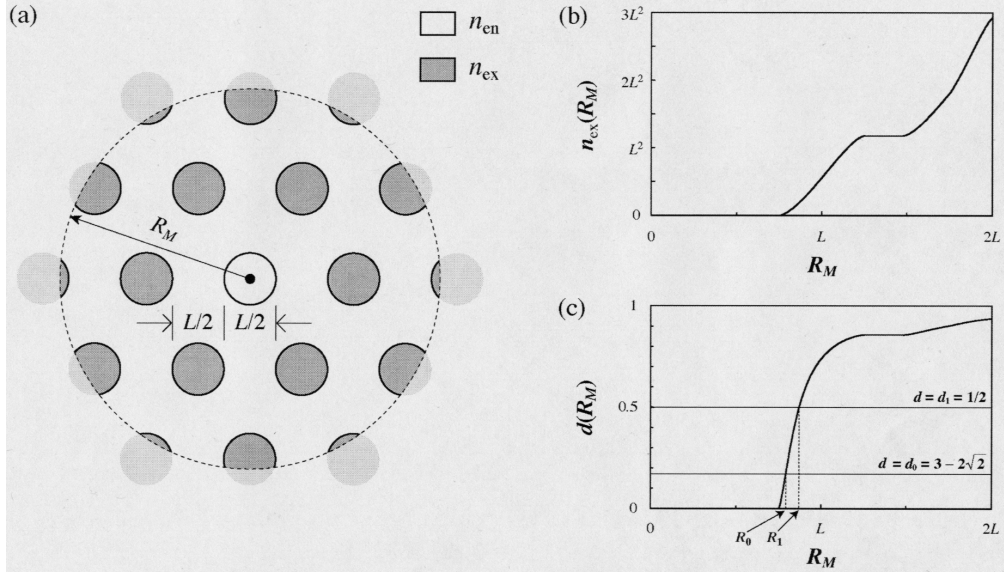
Fig. 4. (a) Illustration of the idealized group distribution assumed to compute d as a function of $\gamma = R_M/R_C$. The isolated groups are assumed to be arranged on a regular hexagonal lattice with basis vectors of length L and group diameter $L/2$. The population distribution is assumed to be flat within a group and thus the total population of a region is proportional to the populated area. n_{en} is the area of the central white circle ($n_{en} = \pi(L/4)^2$), while n_{ex} is the total area of the gray regions. (b) A plot of n_{ex} as a function of R_M, drawn based on analytical calculation using the assumptions in (a). (c) A plot of d as a function of R_M, drawn from (b). Two critical points $d = d_0 = 3 - 2\sqrt{2}$ and $d = d_1 = 1/2$ are shown with the corresponding R_M values R_0 and R_1.

a group is uniform. With these assumptions, n_{en} is the circular area shown by white, and n_{ex} is the area shown by gray, in the figure. $n_{en} = \pi(L/4)^2$ for $R_M > L/4$. The algebraic solution gives $n_{ex}(R_M)$ plotted in Fig. 4(b), and $d(R_M)$ plotted in Fig. 4(c). The critical values of R_M such that $d = d_0 = 3 - 2\sqrt{2}$ and $d = d_1 = 1/2$, which we call R_0 and R_1, are also shown. Numerically we obtain

$$R_0 \approx 0.791234L \approx 0.968R_C \equiv \gamma_0 R_C, \tag{39}$$

$$R_1 \approx 0.869629L \approx 1.06R_C \equiv \gamma_1 R_C, \tag{40}$$

where the coefficients before R_C are the corresponding values of γ, which we call γ_0 and γ_1. Finally, we note that γ_c computed in the flat fitness case still applies to the disruptive selection case with no modification. The analysis discussed here applies to spot patterns. A similar analysis may be done for the stripe patterns that occur for small $\hat{\delta}$ (see Fig. 1).

Using the above results, the following scenario describes the role of γ in the genetic invasion processes in the disruptive selection case:
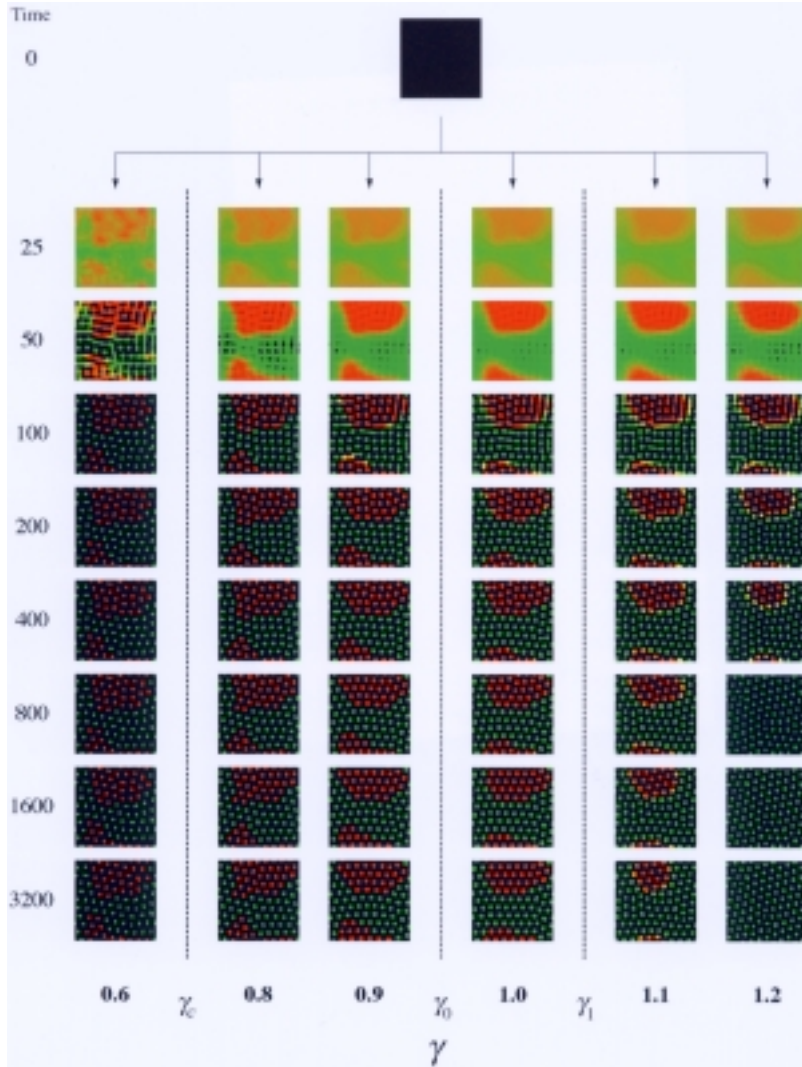
Fig. 5. Numerical simulations of pattern formation in both population distribution and type difference for several different values of γ in the disruptive selection case. The space consists of 128×128 sites with periodic boundary conditions. Red represents the existence of [++] organisms, green represents the existence of [−−], and black represents empty (or nearly empty) regions. $\sigma = 0.9$ and $\lambda = 3.0$ so that $\hat{\delta} = 14$. R_C is fixed to 10, while R_M is varied to obtain different values of γ. The initial condition is a randomly generated population with $n = 0.1\kappa$ (with $\pm 0.02\kappa$ fluctuations) for each site. The same initial condpition is used for all cases to clarify the difference of behaviors for different γ. For $\gamma < \gamma_c \approx 0.612$, complete genetic decoupling occurs once groups are fully isolated from each other. For $\gamma_c < \gamma < \gamma_0 \approx 0.968$, groups are effectively decoupled once they approach dominance by one of the two types (after about 200 updates). In contrast, for $\gamma > \gamma_1 \approx 1.06$, coarsening continues after the isolation of groups, leading to eventual dominance of the whole population by one type. Between these regimes ($\gamma_0 < \gamma < \gamma_1$) there is a distinct behavior where coarsening continues after the isolation of groups but stops when the local curvature of boundaries becomes below a threshold.
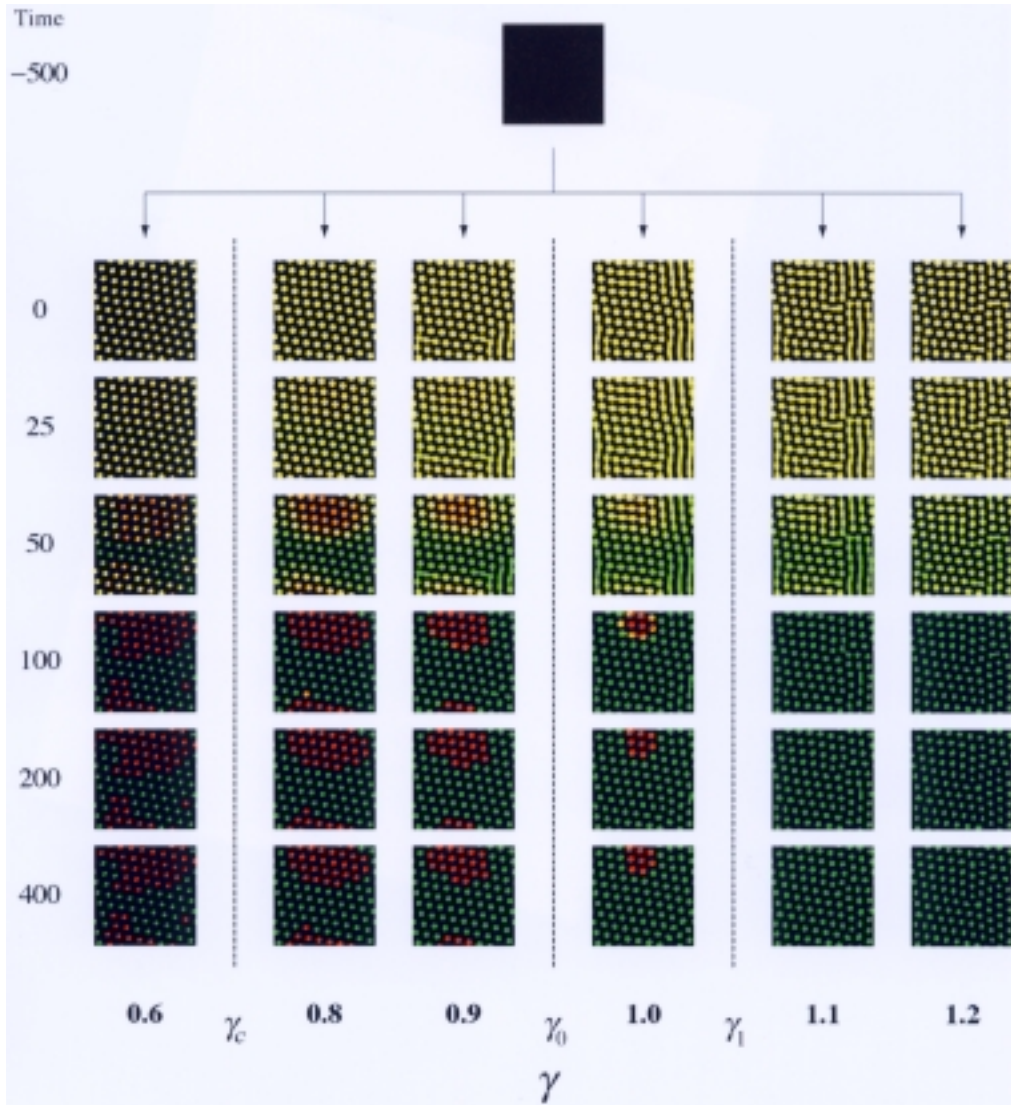
Fig. 6. Numerical simulations of pattern formation in type difference where disruptive selection is induced in a population which is already structured into isolated groups. As in Fig. 5, red, green and black indicate [++], [−−] and empty regions, respectively. Yellow represents a mixed population of all the possible genotypes. R_C is fixed to 10, while R_M is varied to obtain different values of γ. The conditions shown at time 0 are generated through 500 updates with $\sigma = 0.9$ and $\lambda = 1.5$ for all four genotypes (i.e. no disruptive selection) starting from the same initial population as used in Fig. 5. At time 0 the four possible genotypes all co-exist in yellow groups. Then σ_{+-}, σ_{-+}, λ_{+-} and λ_{-+} are all set to zero to cause disruptive selection, while λ_{++} and λ_{--} are increased to 3.0 to make $\hat{\delta}$ after the introduction of disruptive selection equal to δ before the introduction of disruptive selection. The behavioral difference between cases $\gamma < \gamma_0$ and $\gamma > \gamma_1$ appears earlier than the corresponding cases in Fig. 5, while the final outcomes are similar to those in Fig. 5.

For $\gamma < \gamma_c$ (complete decoupling):

Once spatial separation of groups takes place, organisms in one group are genetically decoupled from the rest of the population and each group's genetic composition evolves independently. This corresponds to the case where $d = 0$.

For $\gamma_c < \gamma < \gamma_0$ (incomplete decoupling):

Some inter-group influence occurs, however, effective genetic decoupling between the groups occurs as soon as each of them becomes dominated by either of the two fittest types. A change from one dominant type to another is not possible.

For $\gamma_0 < \gamma < \gamma_1$ (incomplete coarsening):

Coarsening occurs to some extent, but boundaries with curvatures below a threshold remain.

For $\gamma_1 < \gamma$ (complete coarsening):

Genetic invasion always occurs and coarsening continues until all boundaries are flat or one type dominates the entire population.

These results are confirmed in Fig. 5, which presents numerical simulations in the disruptive selection case with several different values of γ, starting with the initial conditions that are randomly created with small fluctuations in both population distribution and genetic distribution. The effects of spatial separation on the domain coarsening behavior in type difference are seen to vary for different γ. For $\gamma < \gamma_0$, genetic decoupling actually occurs and thus coarsening stops after groups become fully isolated from each other (after about 200 updates), while for $\gamma > \gamma_1$, coarsening continues even after the isolation of groups and the whole population is eventually dominated by one type as predicted. Although this particular example does not clearly show how boundaries behave for $\gamma_0 < \gamma < \gamma_1$, we can nonetheless observe a distinct behavior in other simulation runs where coarsening continues after the isolation of groups but eventually stops in a somewhat frustrated shape. Figure 6 shows another example, where isolated groups are already formed when disruptive selection events are induced. In this case, the difference between the cases $\gamma < \gamma_0$ and $\gamma > \gamma_1$ appears earlier due to the pre-existence of the spatial separation. The final outcomes are similar to those in Fig. 5.

7. Conclusion

We have presented a theoretical analysis of evolutionary processes that involve organism distribution, genetic distribution, and their interaction, for spatially distributed populations with local mating and competition. Analyses and numerical simulations reveal that the typical dynamics of population distribution variation is the formation of isolated groups (spots or stripes). This process depends on several parameters, including the reproduction rate and the survival rate of organisms and the ratio of mating and competition ranges. We have also found that the population distribution dynamics are sensitive to the shape of neighborhoods adopted. With well-defined competition neighborhoods groups may form, while with Gaussian neighborhoods they do not. This result implies that the spontaneously formed spatial population structure depends on the organismal behavior in marking their territories.

Then we have examined the dynamics of genetic distribution in the presence of disruptive selection against genetic intermediates. This results in symmetry breaking and

domain coarsening in type difference. The genetic invasion processes may take place despite the spatial separation generated by competition. The ratio of the mating and competition ranges plays a crucial role in the dynamics. Our analysis predicts that there are three distinct critical values of γ, at which the behavior changes from complete decoupling to incomplete decoupling to incomplete coarsening to complete coarsening. In particular, in the incomplete coarsening regime where $\gamma \approx 1$ ($R_M \approx R_C$), the coarsening of boundaries between different types may remain in a frustrated shape. These results are confirmed by numerical simulations. They may be verified by experimental observations in both qualitative and quantitative ways.

There are a number of possible future extensions of the present model. We have considered more complex genetics with multiple loci and/or multiple alleles (SAYAMA *et al.*, 2003). Another issue relevant to biological concerns is extending the fitness assignment to a more general form. A small asymmetry between fittest types or small viability of genetic intermediates may alter the model dynamics. Boundary shapes and behaviors could couple to fitness variation. Our discussions may also be used as an analog of some self-organization processes in physics that involve two or more order parameters, such as clustering and magnetization of aggregates of mobile spins on a two-dimensional surface, or pattern formation of chemical substrates in a reaction-diffusion system that involves multiple distinct reaction processes.

REFERENCES

BRAY, A. J. (1994) Theory of phase-ordering kinetics, *Adv. Phys.*, **43**, 357–459.

DE AGUIAR, M. A. M., SAYAMA, H., RAUCH, E., BAR-YAM, Y. and BARANGER, M. (2002) Stability and instability of polymorphic populations and the role of multiple breeding seasons in phase III of Wright's shifting balance theory, *Phys. Rev. E*, **65**, 031909, 7 pages.

DIECKMANN, U. and DOEBELI, M. (1999) On the origin of species by sympatric speciation, *Nature* (London), **400**, 354–357.

GANDHI, A. S., LEVIN, S. and ORSZAG, S. (1998) "Critical slowing down" in time-to-extinction: an example of critical phenomena in ecology, *J. theor. Biol.*, **192**, 363–376.

GANDHI, A. S., LEVIN, S. and ORSZAG, S. (1999) Nucleation and relaxation from meta-stability in spatial ecological models, *J. theor. Biol.*, **200**, 121–146.

KONDRASHOV, A. S. and KONDRASHOV, F. A. (1999) Interactions among quantitative traits in the course of sympatric speciation, *Nature* (London), **400**, 351–354.

LEVIN, S. A. and SEGEL, L. A. (1985) Pattern generation in space and aspect, *SIAM Rev.*, **27**, 45–67.

MURRAY, J. D. (1981) A prepattern formation mechanism for animal coat markings, *J. theor. Biol.*, **88**, 161–199.

SAYAMA, K., KAUFMAN, L. and BAR-YAM, Y. (2000) Symmetry breaking and coarsening in spatially distributed evolutionary processes including sexual reproduction and disruptive selection, *Phys. Rev. E*, **62**, 7065–7069.

SAYAMA, H., DE AGUIAR, M. A. M., BAR-YAM, Y. and BARANGER, M. (2002) Spontaneous pattern formation and genetic invasion in locally mating and competing populations, *Phys. Rev. E*, **65**, 051919, 15 pages.

SAYAMA, H., KAUFMAN, L. and BAR-YAM, Y. (2003) Spontaneous pattern formation and genetic diversity in habitats with irregular geographical features, *Conserv. Biol.* (in press).

THODAY, J. M. (1972) Disruptive selection, *Proc. R. Soc. London, Ser. B*, **182**, 109–143.

TURING, A. (1952) The chemical basis of morphogenesis, *Philos. Trans. R. Soc. London B*, **237**, 37–72.

YOUNG, D. A. (1984) A local activator-inhibitor model of vertebrate skin patterns, *Mathematical Biosciences*, **72**, 51–58.